Journal of Solid State Chemistry **168,** 535–546 (2002)
doi:10.1006/jssc.2002.9751

Charge Carrier Doping in the Ni(dmit)$_2$ Simple Salts by Hydrogen-Bonding Pyridinium Cations (dmit=1,3-dithiol-2thione-4,5-dithiolate)

Takeshi Hirose, Hiroyuki Imai,[1] Toshio Naito, and Tamotsu Inabe[2]

Division of Chemistry, Graduate School of Science, Hokkaido University, Sapporo 060-0810, Japan

Received January 8, 2002; in revised form April 15, 2002; accepted April 19, 2002

Three kinds of the 1:1 Ni(dmit)$_2$ salts with 4-(4-pyridyl)pyridinium (PP), 4-[2-(4-pyridyl)ethenyl]pyridinium (P=P), and 4-[2-(4-pyridyl)ethyl]pyridinium (P–P) cations have been prepared and structurally characterized. All of these crystals are composed of a multi-dimensional network of the Ni(dmit)$_2$ anions and the hydrogen-bonding one-dimensional cation chains. Compared with tight hydrogen bonds in the P=P and P–P chains, that in the PP chain is rather loose. The P=P and P–P salts show semiconducting behavior with high resistivity and large activation energy, while the PP salt shows the opposite temperature dependence with low resistivity at high temperature. The thermoelectric power indicates that the PP salt is an *n*-doped semiconductor. The proton defects may occur in the loosely bound PP chain which results in the carrier doping in the conduction band formed by the π–π interaction of the Ni(dmit)$_2$ anion radicals.

Key Words: **Ni(dmit)$_2$; pyridinium cation; crystal structure; electrical conductivity; doped semiconductor; hydrogen bond.**

1. INTRODUCTION

The metal–dithiolate complex, Ni(dmit)$_2$, is an excellent building block of electronic functional materials (1). The complex can take various oxidations states from −2 to 0, and their mixed valence compounds were found to be metallic conductors and superconductors. When Ni(dmit)$_2$ is in the mono-anionic state, the unpaired electron is distributed over the whole molecule. The crystal containing only such a π-radical anion species (simple salt) is generally a semiconductor or an insulator due to the on-site Coulomb repulsion energy which is usually greater than the band width formed by the overlaps of the frontier orbitals. Sometimes, the π-radical forms a dimeric unit in the crystal so that the band gap opens at the Fermi level in the half-filled band. This is also expected to lead to the insulating nature in the charge transport.

On the other hand, it is notable that the dimer formation in the simple salts is driven by the strong antiferromagnetic exchange interaction between the π-radicals. This suggests that the Ni(dmit)$_2$ mono-anion can be viewed from a building block of magnetic materials. Indeed, the molecular spin-ladder system was discovered by combining the Ni(dmit)$_2$ anion radical with the *p*-EPYNN (*p*-*N*-ethylpyridinium α-nitronyl nitroxide) cation (2,3). In this crystal, each of the plane-to-plane overlapped dimeric unit of the Ni(dmit)$_2$ anion radicals becomes a rung of the ladder, and two legs are formed by the translational array of the dimeric units. Since the antiferromagnetic two-leg spin ladder attracts attention due to a possibility of the superconducting state by charge carrier doping, the next step may be to dope in *p*-EPYNN[Ni(dmit)$_2$]. There may be two ways of doping; one is replacement of *p*-EPYNN with a dopant possessing a different charge, and another is insertion of a dopant in the interstitial sites of the lattice. Both methods were attempted, but found to be extremely difficult. Then more flexible units for doping have been adopted as the cationic component. 4,4′-Dipyridyl-type framework may be a promising precursor, since the valency can be tuned by the degree of protonation. In addition, when the singly protonated cation is used as the cationic component, one-dimensional chain formation is expected to occur in their salt crystals by the inter-molecular N–H···N hydrogen bond, which may be utilized for the lattice design. The one-dimensional chain structure of the cationic component appears to be one of the key features of the ladder formation as found in *p*-EPYNN[Ni(dmit)$_2$].

[1] Present address: Institute for Molecular Science, Okazaki 444-8585, Japan.

[2] To whom correspondence should be addressed. Fax: +81 11-706-4924. E-mail: inabe@sci.hokudai.ac.jp.

0022-4596/02 $35.00

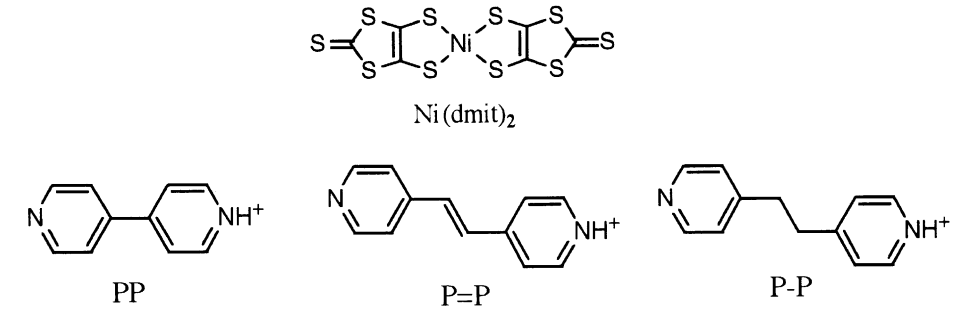

SCHEME 1.

In this paper, the crystal structures and electrical properties of three simple salts, $(PP)_2[Ni(dmit)_2]_2(TCE)$ (TCE = 1,1,2-trichloroethane), $(P{=}P)_2[Ni(dmit)_2]_2(ClPh)$ (ClPh = chlorobenzene), and P–P[Ni(dmit)$_2$], are presented (Scheme 1). Their electrical properties have been found to depend on the strength of the hydrogen bonds between the cations. When the hydrogen bond is not so tight, proton defects may occur which leads to the charge carrier doping.

2. EXPERIMENTAL

2.1. Materials

Three simple salt crystals of Ni(dmit)$_2$ were prepared by the slow-diffusion metathesis between *n*-$Bu_4N[Ni(dmit)_2]$ and the PF_6 salts of the pyridinium cations in the H-tube at 22°C. The solvent system used was acetonitrile/TCE (1:1) for the PP salt, acetonitrile/ClPh (1:1) for the P=P salt, and acetonitrile for the P–P salt. The PF_6 salts of the pyridinium cations were prepared by the reaction of the precursors (4,4′-dipyridyl, *trans*-1,2-bis(4-pyridyl)ethylene, and 1,2-bis(4-pyridyl)ethane) with equimolar HCl followed by the metathesis using NH_4PF_6.

2.2. X-Ray Structure Analyses

A Rigaku R-AXIS Rapid imaging plate diffractometer with graphite-monochromated Mo$K\alpha$ radiation was used for data collection, and the crystal data are summarized in Table 1. The structures were solved by a direct method (SIR-92 (4)), The hydrogen atoms attaching to carbon were placed at the calculated ideal positions, and their coordinates were not refined. The positions of hydrogen atoms in the hydrogen bonds were determined by the difference

TABLE 1
Crystal data of $(PP)_2[Ni(dmit)_2]_2(TCE)$, $(P{=}P)_2[Ni(dmit)_2]_2(ClPh)$, and (P–P)[Ni(dmit)$_2$]

	$(PP)_2[Ni(dmit)_2]_2(TCE)$	$(P{=}P)_2[Ni(dmit)_2]_2(ClPh)$	P–P[Ni(dmit)$_2$]
Chemical formula	$C_{34}H_{21}N_4S_{20}Ni_2Cl_3$	$C_{42}H_{27}N_4S_{20}Ni_2Cl$	$C_{18}H_{13}N_2S_{10}Ni$
Molecular weight	1350.53	1381.86	636.61
Temperature (K)	293	108	108
Crystal system	Triclinic	Triclinic	Triclinic
Space group	$P\bar{1}$(#2)	$P\bar{1}$(#2)	$P\bar{1}$(#2)
a (Å)	11.868(1)	12.131(1)	16.889(2)
b (Å)	19.273(2)	14.190(1)	23.051(1)
c (Å)	11.668(1)	8.125(1)	9.201(1)
α (deg)	102.18(1)	97.07(1)	93.30(1)
β (deg)	95.29(1)	90.49(1)	94.53(1)
γ (deg)	105.47(1)	69.04(1)	88.39(1)
V (Å^3)	2482.8(3)	1295.1(2)	3564.1(5)
Z	2	1	6
D_{calc} (g cm^{-3})	1.806	1.772	1.779
Number of reflections measured	10683	5594	15035
Number of reflections observed	5982	3889	6190
	$[F_o^2 > 2.0\sigma(F_o^2)]$	$[F_o^2 > 3.0\sigma(F_o^2)]$	$[F_o^2 > 3.0\sigma(F_o^2)]$
R_{int}	0.04	0.04	0.05
Number of parameters	574	346	847
Goodness of fit	2.72	1.49	1.35
R	0.055	0.040	0.048
R_w	0.044	0.054	0.053

TABLE 2
Bond Lengths (Å) for $Ni(dmit)_2$

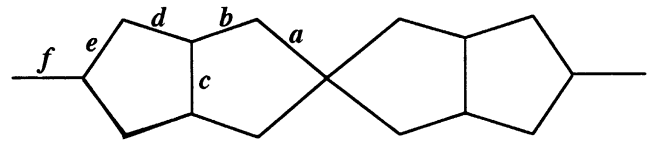

	$(PP)_2[Ni(dmit)_2]_2$-(TCE)			P–P[Ni(dmit)$_2$]			$(n\text{-}Bu_4N)_n$-[Ni(dmit)$_2$]	
Bond	*A*	*B*	$(P{=}P)_2[Ni(dmit)_2]_2$-(ClPh)	*A*	*B*	*C*	$n=1$[a]	$n=2$[a]
a	2.164	2.166	2.160	2.157	2.157	2.160	2.156	2.216
b	1.706	1.716	1.710	1.702	1.713	1.710	1.73	1.75
c	1.371	1.370	1.371	1.38	1.39	1.37	1.35	1.39
d	1.747	1.737	1.736	1.742	1.728	1.735	1.74	1.72
e	1.736	1.728	1.730	1.737	1.729	1.739	1.74	1.74
f	1.634	1.643	1.645	1.634	1.646	1.629	1.63	1.68

[a] Ref. (8).

Fourier syntheses. When only one peak was found in the hydrogen bond, the positional parameters of the H atom were refined. When two peaks were found, the positional parameters were fixed at the peak position with occupancy $=\frac{1}{2}$. A full-matrix least-squares technique with anisotropic thermal parameters for non-hydrogen atoms and isotropic ones for hydrogen atoms was employed for the structure refinement using the teXsan program package (5). The thermal parameters were refined for the hydrogen-bonding H atoms and were fixed for the other H atoms as 1.2 times of that of the attached carbon.

2.3. Measurements

Infrared spectra were measured for the KBr disc samples by a Perkin-Elmer 1600 FT-IR spectrometer. Magnetic susceptibility of $(PP)_2[Ni(dmit)_2]_2$(TCE) was measured in a field of 1 T on a Quantum Design MPMS-5S SQUID susceptometer. The correction of the diamagnetic core contributions was estimated from the value reported for $Ni(dmit)_2$ (6), the experimental value of $PP \cdot PF_6$ for PP cation, and the Pascal's law for TCE. The room-temperature single-crystal conductivities were performed with a four-probe method for the three salts. This method was used for the temperature dependence measurement for $(PP)_2[Ni(dmit)_2]_2$(TCE), and the method was changed to a two-probe one for high resistance $(P{=}P)_2$[Ni (dmit)$_2$]$_2$(ClPh) and P–P[Ni(dmit)$_2$]. It was confirmed that the contact resistance was negligibly small by the comparison between the room-temperature values obtained by the two methods. Thermoelectric power of $(PP)_2$[Ni (dmit)$_2$]$_2$(TCE) was measured for the single-crystal specimen by a similar method reported (7).

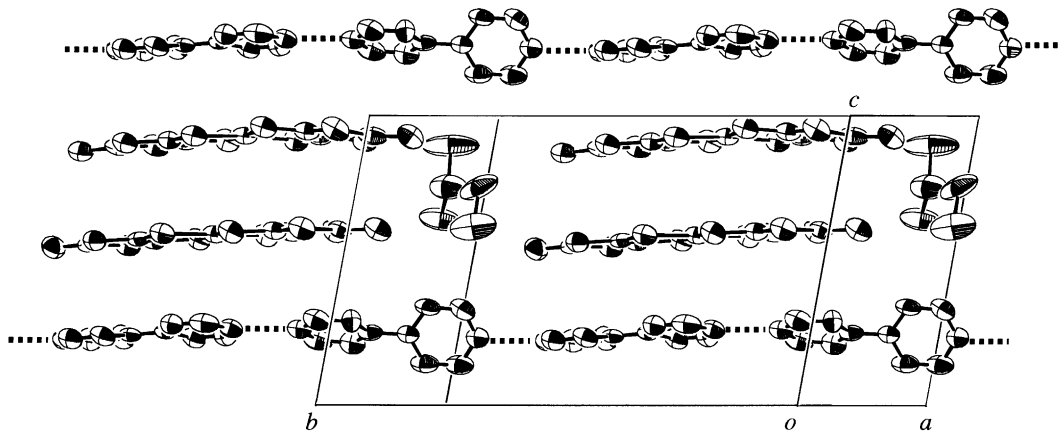

FIG. 1. Molecular arrangement in the lattice of $(PP)_2[Ni(dmit)_2]_2$(TCE).

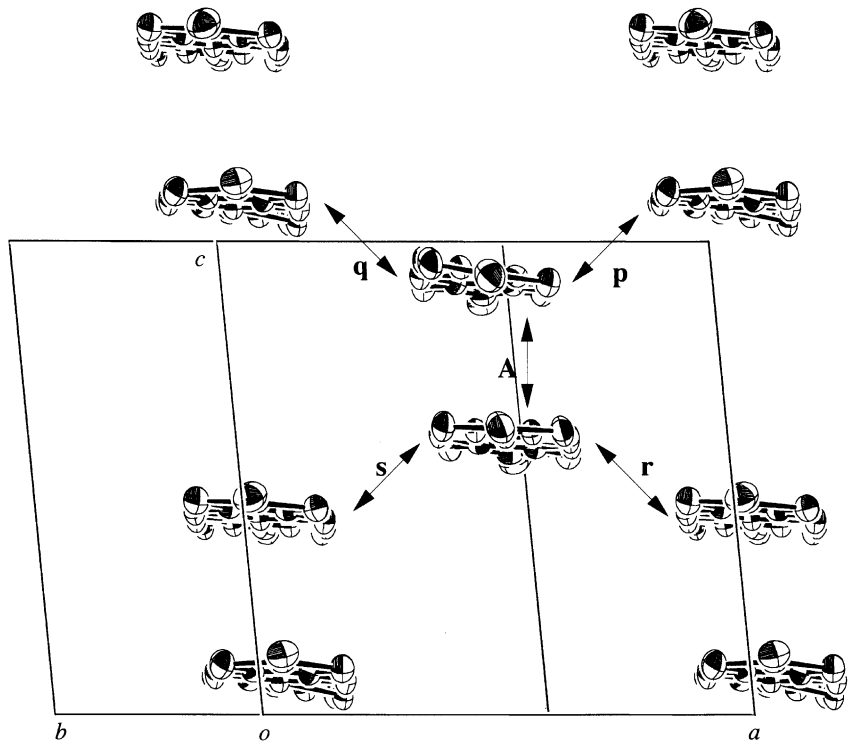

FIG. 2. Two-dimensional arrangement of $Ni(dmit)_2$ in the *ac* plane of $(PP)_2[Ni(dmit)_2]_2(TCE)$.

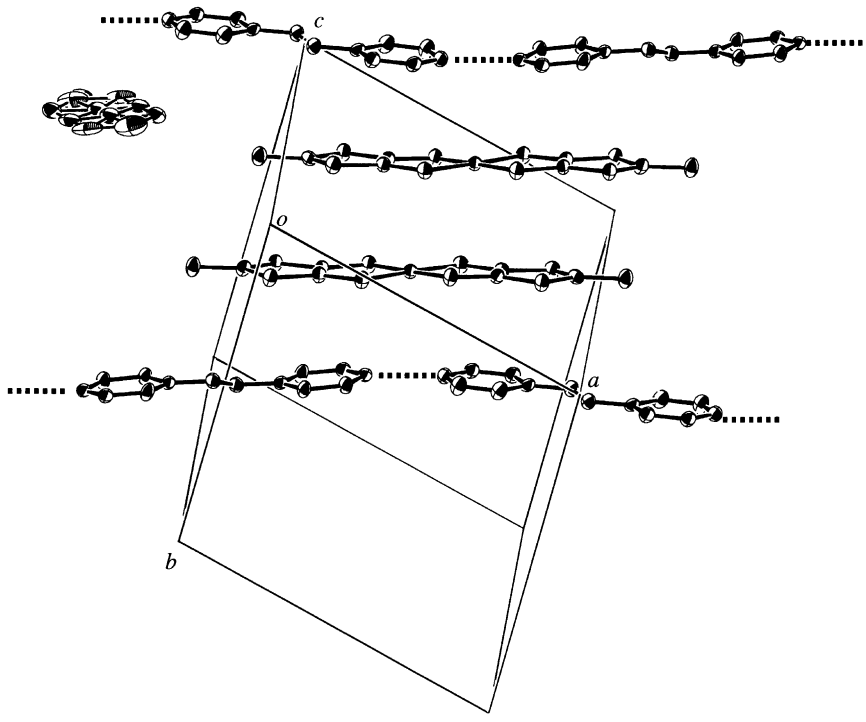

FIG. 3. Molecular arrangement in the lattice of $(P{=}P)_2[Ni(dmit)_2]_2(ClPh)$.

3. RESULTS AND DISCUSSION

3.1. Crystal Structures

3.1.1. Crystal structure of (PP)$_2$[Ni(dmit)$_2$]$_2$ (TCE). The assymmetric unit in this crystal contains two Ni(dmit)$_2$, two PP, and one TCE. As shown in Table 2, the difference of the bond lengths between the two cry-stallographically independent Ni(dmit)$_2$ molecules is small. The bond ***a*** is known to be sensitive to the formal charge of Ni(dmit)$_2$ (8). Though the values look slightly larger compared with that in *n*-Bu$_4$N[Ni(dmit)$_2$], they are still in the range of that in the mono-anion (standard deviations are about 0.004 Å) and far from that in [Ni(dmit)$_2$]$^{2-}$.

The molecular arrangement is shown in Fig. 1. The PP cations form a one-dimensional chain along the *b*-axis by the N–H$\cdots$N hydrogen bonds (2.774(8)) and 2.725(8) Å). The Ni(dmit)$_2$ anions form a plane-to-plane overlapped dimeric unit (interplanar distance: 3.69 Å). The dimeric units are sandwiched between the PP chains. The PP cation over the Ni(dmit)$_2$ anion is relatively planar (dihedral angle between the two pyridine rings is 12.2°), while that bridging them is distorted (dihedral angle is 49.1°). The Ni(dmit)$_2$ arrangement in the *ac* plane is shown in Fig. 2. Along the *c*-axis, the Ni(dmit)$_2$ dimers are separated by the PP chains (Fig. 1). On the other hand, the side-by-side interaction between the Ni(dmit)$_2$ molecules is possible along the [101] and [10$\bar{1}$] directions. TCE locates between the Ni(dmit)$_2$ dimers translationally arranged along the *b*-axis (Fig. 1), so that the interaction along this direction becomes small.

3.1.2. Crystal structure of (P=P)$_2$[Ni(dmit)$_2$]$_2$ (ClPh). The assymmetric unit in this crystal contains one Ni(dmit)$_2$, two halves of the P=P unit, and one-half of ClPh. This crystal has several common features observed for the structure of (PP)$_2$[Ni(dmit)$_2$]$_2$(TCE); mono-anionic molecular geometry of Ni(dmit)$_2$ (Table 2), hydrogen-bonded one-dimensional chain formation of P=P (along the [2$\bar{1}$0] direction), plane-to-plane dimer formation of Ni(dmit)$_2$ (inter-planar distance: 3.57 Å), and sandwich of the Ni(dmit)$_2$ dimer unit by the P=P chains (Fig. 3). The N–H$\cdots$N hydrogen bond in the P=P chain (2.616(5) Å) is

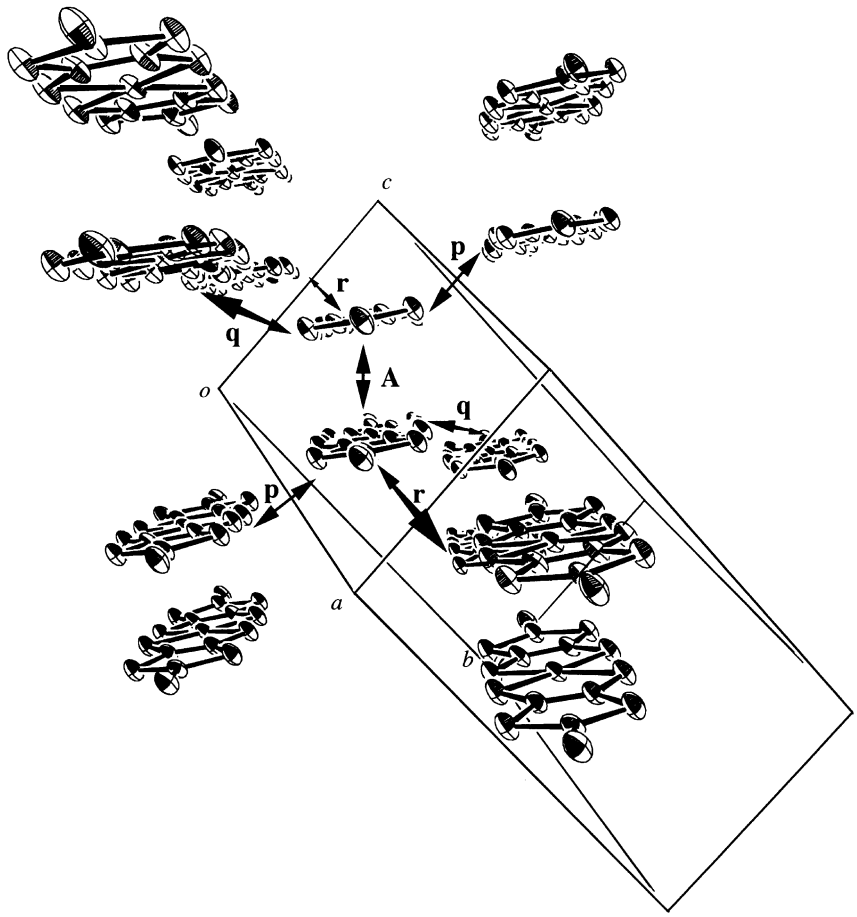

FIG. 4. Intermolecular interactions between the Ni(dmit)$_2$ units in (P=P)$_2$[Ni(dmit)$_2$]$_2$(ClPh).

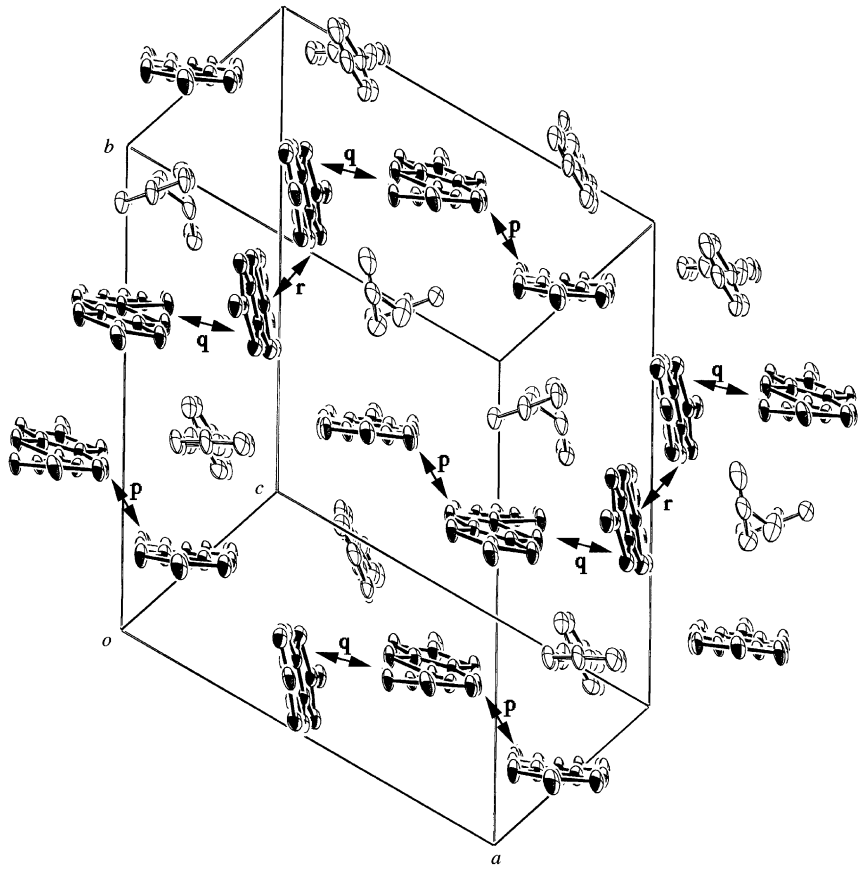

FIG. 5. Molecular arrangement in the lattice of P–P [Ni(dmit)$_2$]; molecules with shaded ellipsoids are Ni(dmit)$_2$.

much stronger than that in (PP)$_2$[Ni(dmit)$_2$]$_2$(TCE). The P═P cations are practically planar, and they are nearly coplanar in the chain. The consequently leads to the tightly bound chain. As shown in Fig. 4, The Ni(dmit)$_2$ anions form a multidimensional network through the peripheral S···S contacts. The orientationally disordered ClPh molecules are located between the Ni(dmit)$_2$ dimers (Fig. 3), however, it does not prevent the inter-dimer interaction along the long axis of Ni(dmit)$_2$.

3.1.3. Crystal structure of P–P[Ni(dmit)$_2$]. The asymmetric unit in this crystal containing three Ni(dmit)$_2$ anions and three P–P cations. This crystal has two common features observed for the structures of (PP)$_2$[Ni(dmit)$_2$]$_2$ (TCE) and (P═P)$_2$[Ni(dmit)$_2$]$_2$(ClPh); mono-anionic molecular geometry of Ni(dmit)$_2$ (Table 2) and hydrogen-bonded one-dimensional chain formation of P–P. However, a marked difference lies in the Ni(dmit)$_2$ arrangements; in this crystal the Ni(dmit)$_2$ anions do not form a dimeric unit. This may be because the P–P cation is conformationally more flexible than PP and P═P; P–P has additional freedom of rotation around the central C–C bond. Consequently, two of the three independent P–P cations show large deviations from its planar form (Fig. 5). All the hydrogen bonds in the P–P chain (2.64–2.66 Å) are again considerably stronger than those in the PP chain. The arrangement of the Ni(dmit)$_2$ anions is shown in Fig. 6. Through many short S···S contacts the radical anions form complicated two-dimensional sheets.

3.1.4. Comparison of the one-dimensional cation chains. Three kinds of hydrogen-bonded cation chains are shown in Fig. 7. In the PP chain, one bond is relatively rigid (bond **i**), and the position of the H atom is not disordered. On the other hand, in bond **ii**, two H atoms were found with nearly equal probability (assigned as occupancy = $\frac{1}{2}$). Both H atoms are largely derived from the N···N line, in contrast to almost linear N–H···N alignment in bond **i**. In the P═P chain, one H atom was found around the middle of the hydrogen bond. The N–H–N bond is nearly linear. Its very short N···N distance (2.616(5) Å) corresponds to a strong hydrogen bond, which leads to the elongation of he N–H bond and contraction of the N···H distance (9). Consequently, the H atom situates at a broad minimum in a nearly single-well potential. Since the N···N distance is much shorter than twice that of the

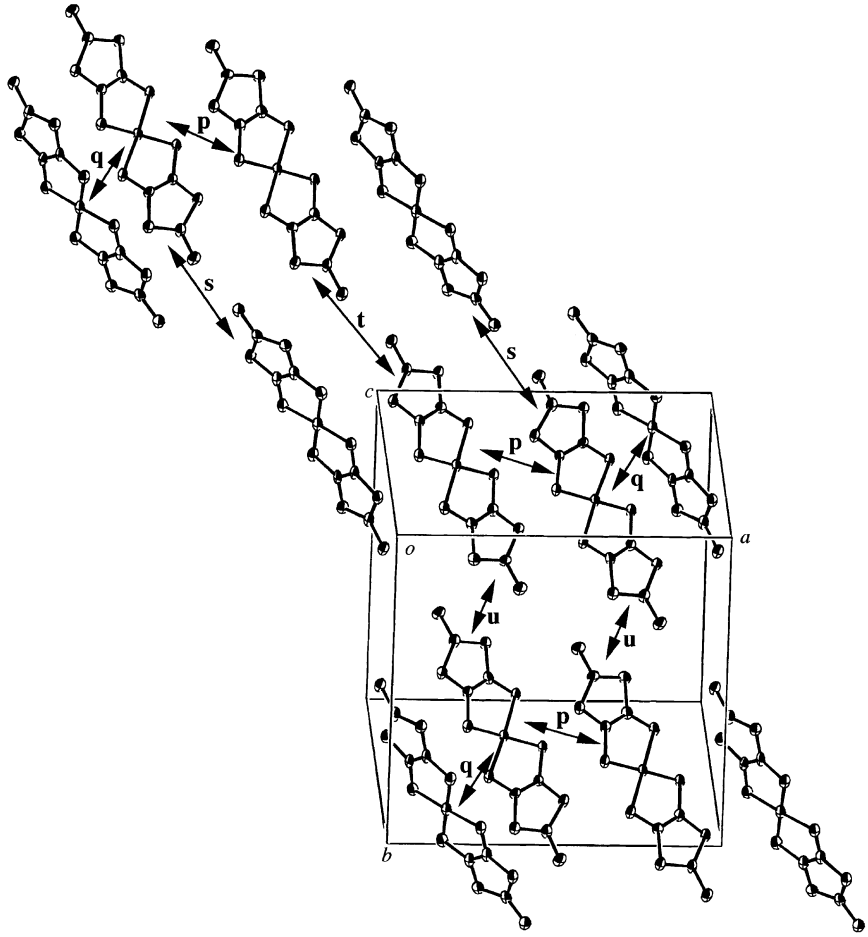

FIG. 6. Intermolecular interactions between the Ni(dmit)$_2$ units in P–P [Ni(dmit)$_2$].

van der Waals radius of nitrogen (3.10 Å), there is little possibility of proton defects in the P═P chain. The situation is almost similar in the P–P chain, only one H atom locates near the midpoint in each N···N line. Again, proton defects are difficult to occur in the P–P chain. Compared with the P═P and P–P chains, the PP chain may have the ability of accommodating proton defects at bond **ii**.

3.2. Physical Properties

3.2.1. Charge transport properties. The temperature dependence of the single-crystal resistivity is shown in Fig. 8(a). Though these three salts have many common structural features, the transport property in the PP salt is significantly different from those in the P═P and P–P salts. High resistivity values with large activation energies (0.21 ~ 0.25 eV) of the P═P and P–P salts are rather normal for the Ni(dmit)$_2$ simple salt. Both dimerized structure (P═P salt) and large on-site Coulomb repulsion energy lead to a large energy gap. It is quite unusual that the PP salt is rather conductive despite the 1:1 stoichiometry. One possibility may be the large band width which surpasses the energy gap. The calculated overlap integrals between the Ni(dmit)$_2$'s frontier orbitals based on the structural data are summarized in Table 3. It is clear that there is no anomalously large overlap in the PP salt. An alternative possibility is the charge carrier doping in the semiconducting PP salt.

Thermoelectric power (S) is useful transport property to elucidate the electronic structure. The temperature dependence of S of (PP)$_2$[Ni(dmit)$_2$]$_2$(TCE) is shown in Fig. 9. It is notable that S has the negative sign and shows nearly temperature-independent values around $-40\,\mu V\,deg^{-1}$ above 180 K. This is a typical behavior of an *n*-doped semiconductor (10). Based on the S behavior, the conductivity data have then been analyzed by the following equation:

$$\rho(T)/\rho(295\ K) = AT^{-\alpha}\exp(-\Delta/kT).$$

As discussed by Epstein *et al.* (11), the temperature dependence of the mobility and that of carrier concentra-

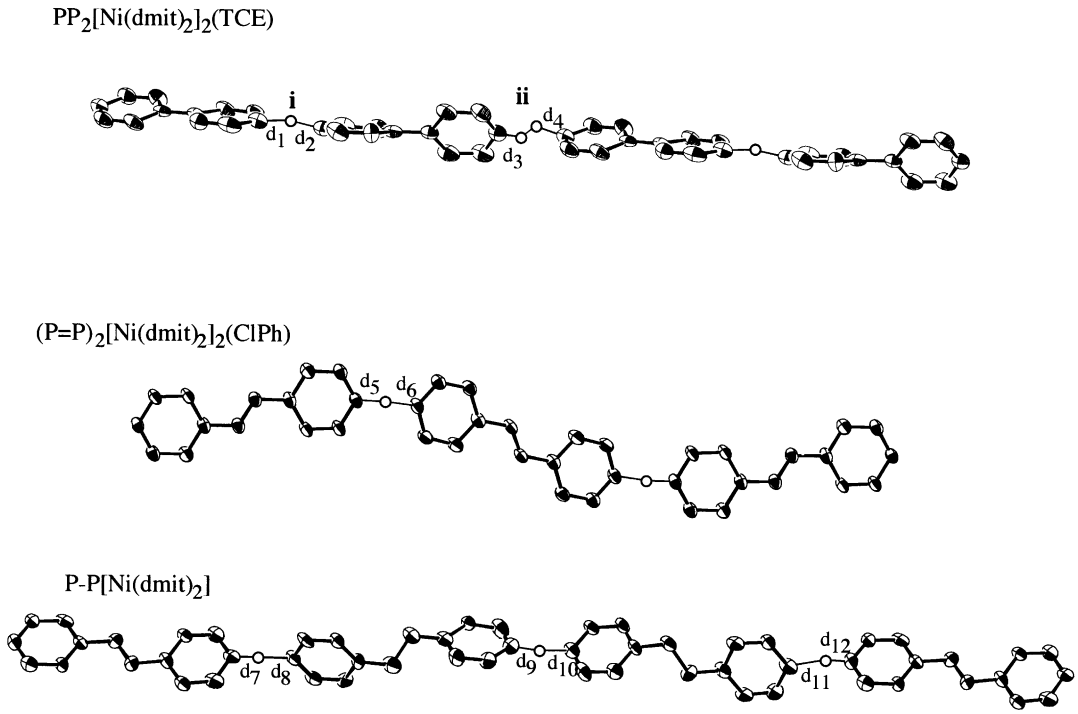

FIG. 7. Comparison of the hydrogen-bonded one-dimensional cation chains; (a) $(PP)_2[Ni(dmit)_2]_2(TCE)$, and (b) $(P{=}P)_2[Ni(dmit)_2]_2(ClPh)$, and (c) $P{-}P[Ni(dmit)_2]$; $d_1 = 1.57(9)$, $d_2 = 1.22(9)$, $d_3 = 0.95(1)$, $d_4 = 1.27(1)$, $d_5 = 1.23(6)$, $d_6 = 1.39(6)$, $d_7 = 1.1(1)$, $d_8 = 1.5(1)$, $d_9 = 1.3(1)$, $d_{10} = 1.4(1)$, $d_{11} = 1.6(2)$, and $d_{12} = 1.2(1)$ Å

tion are proportional to $T^{-\alpha}$ and $\exp(-\Delta/kT)$, respectively. The curve fitting obtained is shown in Fig. 8(b) as a solid line with $\alpha = 1.6$ and $\Delta/k = 353$ K. The agreement is fairly good, and therefore, in $(PP)_2[Ni(dmit)_2]_2(TCE)$, the transport properties indicate that there are *n*-donor levels about 0.06 eV below the bottom of the conduction band. By assuming a typical mobility value in molecular crystals at 300 K ($\sim 1\,cm^2\,V^{-1}\,s^{-1}$), the carrier concentration is calculated to be about $6 \times 10^{17}\,cm^{-3}$. This value corresponds to only 0.04% of the number of constituting Ni $(dmit)_2$ in the unit volume, and the doping level is thus estimated to be $0.1 \sim 0.2\%$. Electron source can be $[Ni(dmit)_2]^{2-}$ generated by the excess cation charge. The excess charge may be accommodated in the hydrogen-bonding PP chain as the excess protonation at bond **ii**.

3.2.2. Magnetic susceptibility of $(PP)_2[Ni(dmit)_2]_2$ (TCE). The temperature dependence of the paramagnetic susceptibility is shown in Fig. 10 (the molar unit is $PP[Ni(dmit)_2](TCE)_{0.5}$). The data show antiferromagnetic exchange interaction operating between the $Ni(dmit)_2$ radicals and some Curie tailing. Though the intermolecular interactions between the $Ni(dmit)_2$ radicals are two dimensional from the overlap integrals (Table 3), they are not isotropic. Since exchange interaction (J) is proportional to t^2 (t is the transfer integral and is proportional to the overlap integral), we can apply an approximation of the one-dimensional antiferromagnetic chain with two alternating interaction parameters J and αJ (12). The data are then analyzed by the sum of contributions from the one-dimensional chain and the Curie–Weiss-type paramagnetism.

$$\chi_p = (4C_1/T)[(A + Bx + Cx^2)/(1 + Dx + Ex^2 + Fx^3)] + C_2/(T - \theta),$$

where x is $|J|/kT$, $A{-}F$ are coefficients including α (12), k is the Boltzmann constant, and θ is the Weiss constant. The best fit in Fig. 10 (solid line) was obtained with $C_1 = 0.367$ emu mol^{-1}, $|J|/k = 237$ K, $\alpha = 0.316$, $C_2 = 0.027$ emu mol^{-1}, and $\theta = -1.9$ K ($C_1 + C_2$ are fixed to

TABLE 3
Overlap Integral Values (10^{-3}) between the $Ni(dmit)_2$ Frontier Orbitals

Intermolecular contract[a]	$(PP)_2[Ni(dmit)_2]_2$-(TCE)	$(P{=}P)_2$-$[Ni(dmit)_2]_2(ClPh)$	P–P_2-$[Ni(dmit)_2]$
A	7.95	17.4	
p	5.09	3.12	1.29
q	1.92	0.48	1.83
r	2.92	2.62	0.75
s	6.46		1.02
t			0.15
u			0.89

[a] Each contact is defined in Figs. 2, 4, 5 and 6.

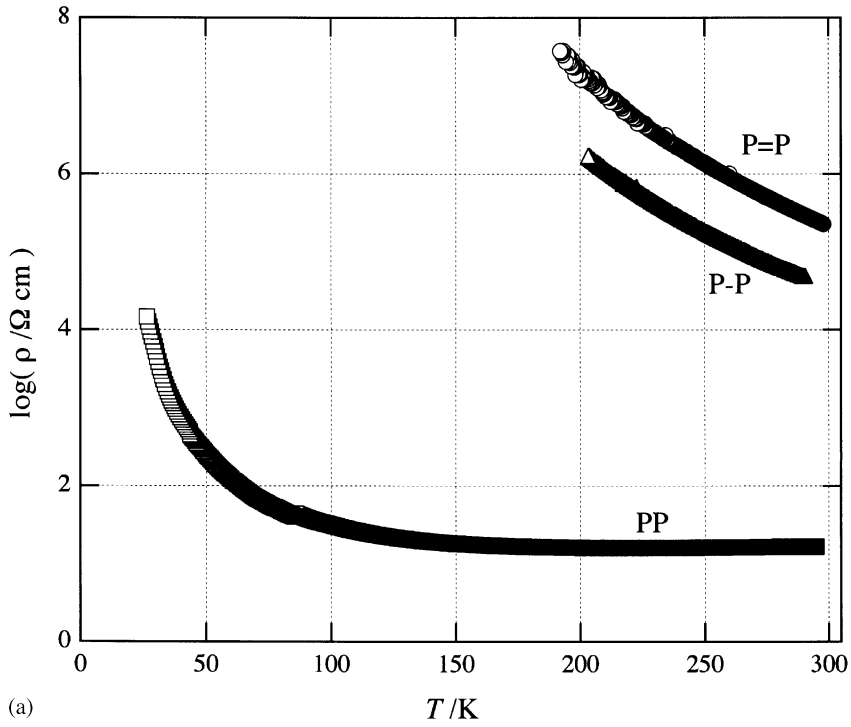

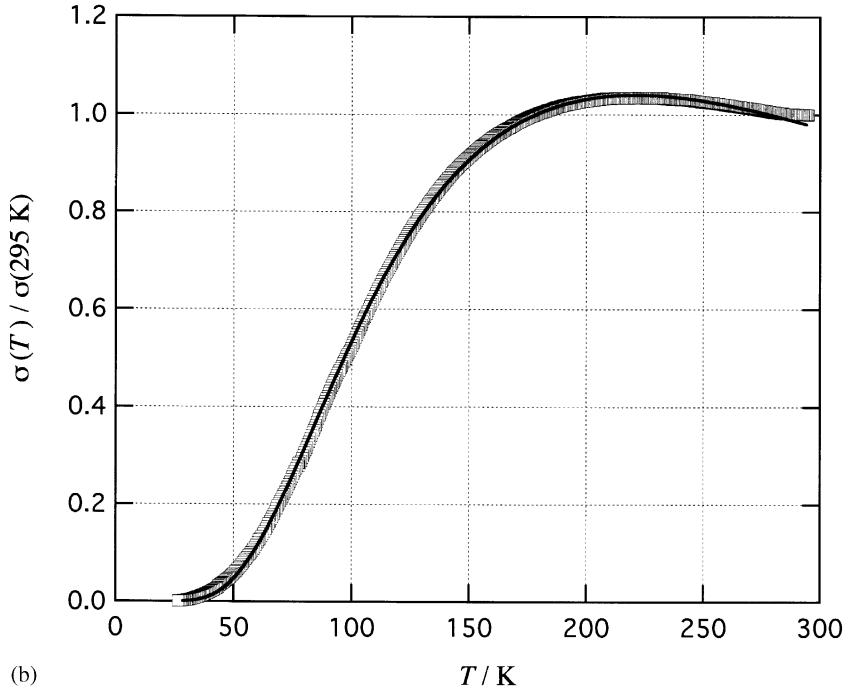

FIG. 8. (a) Temperature dependence of the single crystal resistivity; $\|c$ in P=P, $\|c$ in PP, and $\|c$ in P–P. (b) Temperature dependence of the normalized conductivity of $(PP)_2[Ni(dmit)_2]_2(TCE)$. The solid line is the best fit following the equation in the text.

$0.394\,emu\,mol^{-1}$ for $g = 2.05$ (13)). This picture is qualitatively consistent with the expectation from the transport properties; part of the $Ni(dmit)_2$ mono-anions are replaced by diamagnetic $[Ni(dmit)_2]^{2-}$ which produces the defect sites in the $Ni(dmit)_2$ arrays. It is notable that the number of the defect sites (Curie-type contribution) is much higher than that expected from the transport properties. This probably indicates that the doped $[Ni(dmit)_2]^{2-}$ disturbs the antiferromagnetic coupling to a considerable extent around it.

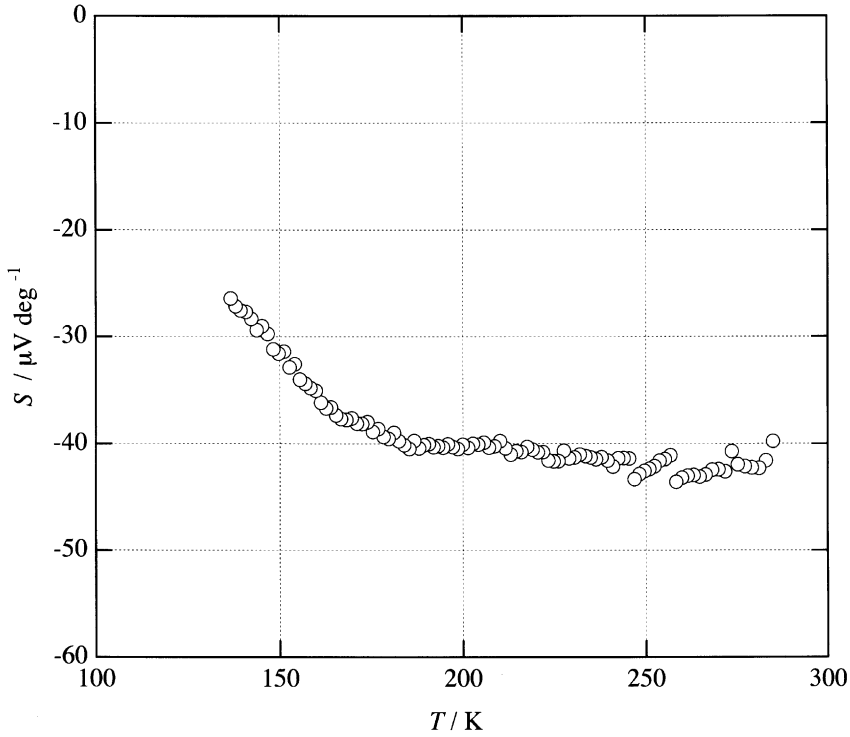

FIG. 9. Temperature dependence of the thermoelectric power (S) of $(PP)_2[Ni(dmit)_2]_2(TCE)$.

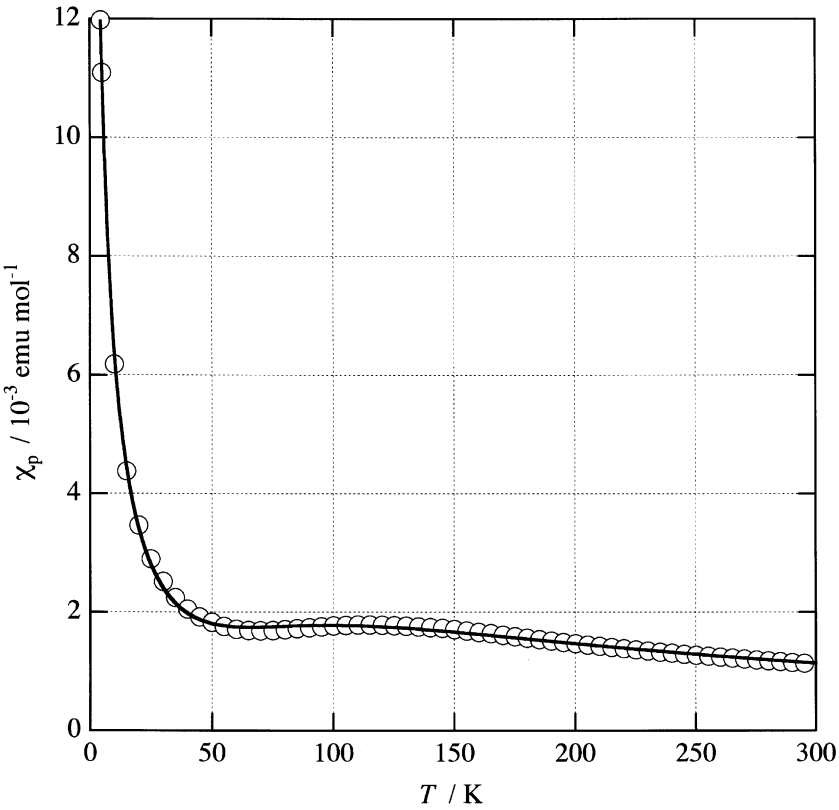

FIG. 10. Temperature dependence of the paramagnetic susceptibility of $(PP)_2[Ni(dmit)_2]_2(TCE)$ (molar unit is $(PP)_1[Ni(dmit)_2]_1(TCE)_{0.5}$). The solid line is the best fit following the equation in the text.

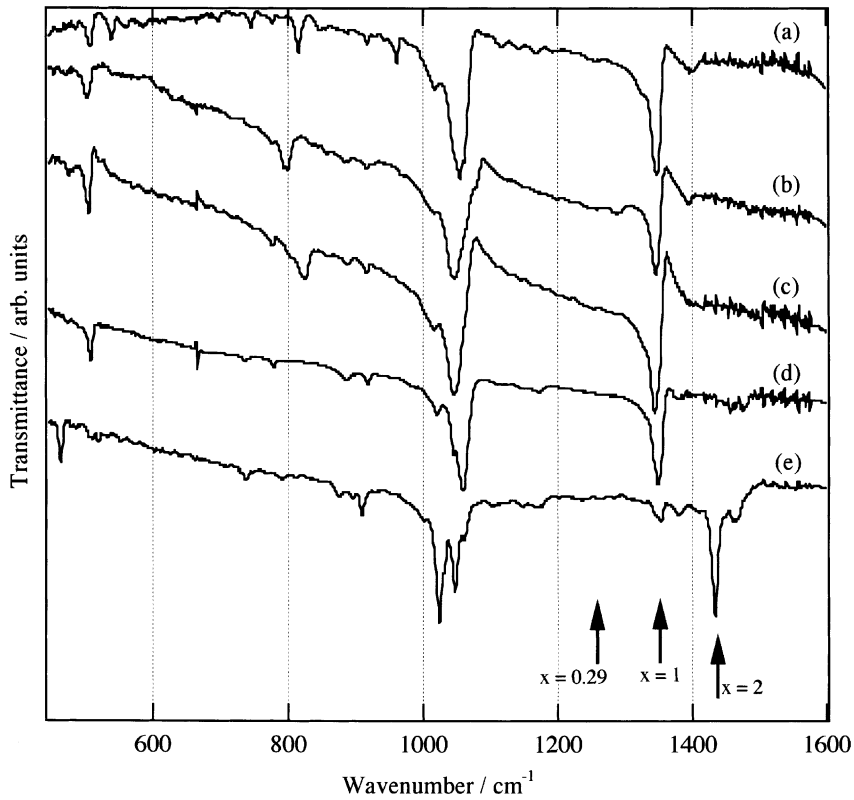

FIG. 11. Infrared spectra of (a) $(PP)_2[Ni(dmit)_2]_2(TCE)$, (b) $(P{=}P)_2[Ni(dmit)_2]_2(ClPh)$, (c) P–P$[Ni(dmit)_2]$ (d) n-$Bu_4N[Ni(dmit)_2]$ and (e) $(n\text{-}Bu_4N)_2[Ni(dmit)_2]$. The arrows indicate the C=C stretching band positions for $(Ni(dmit)_2)^{x-}$.

3.2.3. Infrared spectra. Though the $[Ni(dmit)_2]^{2-}$ species in the PP salt has hardly been detected by X-ray structure analysis, its physical properties suggest the existence of $[Ni(dmit)_2]^{2-}$. Since some vibrational mode is known to be sensitive to the formal charge of $Ni(dmit)_2$, their IR spectra have been examined. The spectra are shown in Fig. 11 together with that of n-$Bu_4N[Ni(dmit)_2]$. The strong band around 1353 cm^{-1} is known as the C=C stretching stretching band of the mono-anion radical, and this band shows large shifts by the formal charge of $Ni(dmit)_2$; 1260 cm^{-1} for $[Ni(dmit)_2]^{0.29-}$ and 1440 cm^{-1} for $[Ni(dmit)_2]^{2-}$ [8]. All the spectra in Fig. 11 clearly show that the $[Ni(dmit)_2]$ unit is a mono-anion. This means that the majority of the ionic species in $(PP)_2[Ni(dmit)_2]_2(TCE)$ are still $(PP)^+$ and $[Ni(dmit)_2]^-$.

3.2.4. Discussion on the doping in $(PP)_2[Ni(dmit)_2]_2$-(TCE). Since S has the negative sign, electrons must be doped in the system. If charge transfer from PP^+ to $[Ni(dmit)_2]^-$ occurs, the $[Ni(dmit)_2]^{2-}$ species may be generated. However, it is highly unlikely, since PP^+ is rather an electron acceptor. It is also supported by the fact that any electron doping effects have not been observed in the P=P salt, though $P{=}P^+$ should have a similar ionization potential with PP^+. Therefore, electron doping must occur through excess protonation which results in co-existence of $[Ni(dmit)_2]^{2-}$ in the crystal. The energy of the frontier orbital of incorporated $[Ni(dmit)_2]^{2-}$ is expected to be slightly different from that of $[Ni(dmit)_2]^-$ which forms the conduction band, due to the difference in the electrostatic potential energy. If the concentration of $[Ni(dmit)_2]^{2-}$ becomes high, the energy difference may be screened. Therefore, the concentration of $[Ni(dmit)_2]^{2-}$ should not be so high, and this is consistent with the fact that the species has little been detected by X-ray structure analysis and by IR spectra. Consequently, in $(PP)_2[Ni(dmit)_2]_2(TCE)$ only a small amount of the incorporated $[Ni(dmit)_2]^{2-}$ species form the donor levels just below the conduction band. The mechanism of the excess protonation may be as follows. In the solution, probably some proton disproportionation occurs; all of the non-protonated, singly protonated, and doubly protonated species may co-exist in the equilibrium state. During the crystallization process, it may be possible for some doubly protonated species to be incorporated in the loosely bound PP chain, while only singly protonated species is selectively incorporated in the tightly bound P=P and P–P chains.

In conclusion, we have found that the electrical conductivity of the $Ni(dmit)_2$ simple salts becomes significantly high when (pyridyl)pyridinium-type counter-

cations form a one-dimensional chain with loose hydrogen bonds. This is probably due to the donor level formation by the excess protonation in the cation chains. Though the salt structures obtained in this study are not of the spin-ladder type, it may be possible to obtain such a structure by properly modifying the PP-type cation. In addition, this study suggests that the doping level may be controlled by adjusting the proton concentration during the crystallization. The study concerning these points is now under way.

ACKNOWLEDGMENTS

This work was partly supported by the Grant-In-Aid for Scientific Research, from the Ministry of Education, Science and Culture, Japanese Government.

REFERENCES

1. P. Cassoux and L. Valade, *in*: "Inorganic Materials" (D. W. Bruce and D. O'Hare Eds.), pp. 2–58. John Wiley & Sons, Chichester, 1992.
2. H. Imai, T. Inabe, T. Otsuka, T. Okuno, and K. Awaga, *Phys. Rev. B* **54,** R6838 (1996).
3. H. Imai, T. Otsuka, T. Naito, K. Awaga, and T. Inabe, *J. Am. Chem. Soc.* **121,** 8098 (1999).
4. A. Altomare, M. C. Burla, M. Camalli, M. Cascarano, C. Giacovazzo, A. Guagliardi, and G. Polidori, *J. Appl. Crystallogr.* **27,** 435 (1994).
5. teXsan, Crystal Structure Analysis Package, Molecular Structure Corporation, 3200 Research Forest Drive, The Woodlands, TX, 1985, 1992.
6. A. E. Underhill, R. A. Clark, I. Marsden, M. Allan, R. H. Friend, H. Tajima, T. Naito, M. Tamura, H. Kuroda, A. Kobayashi, H. Kobayashi, R. Canadell, S. Ravy, and J.-P. Pouget, *J. Phys.: Condens. Matter* **3,** 933 (1991).
7. P. M. Chaikin and J. F. Kwak, *Rev. Sci. Instrum.* **46,** 429 (1975).
8. L. Valade, J.-P. Legros, M. Bousseau, P. Cassoux, M. Garbaskas, and L. V. Interrante, *J. Chem. Soc. Da. Trans.* 783 (1983).
9. W. C. Hamilton and J. A. Ibers, "Hydrogen Bonding in Solids," W. A. Benjamin, Inc., New York, 1968.
10. Another possible model for the constant TEP at high temperature may be a highly correlated metal (P. M. Chaikin and G. Beni, *Phys. Rev. B* **13,** 647 (1976). $S(T\to\infty) = -(e/k)\ln[2(1-\rho)/\rho]$, where ρ is the number of electrons per one site. The observed value ($-40\,\mu V\,deg^{-1}$) gives $\rho = 0.56$, which is unrealistic for $(PP)_2[Ni(dmit)_2]_2(TCE)$.
11. A. J. Epstein, E. M. Conwell, and J. S. Miller, *in*: "Synthesis and Properties of Low-dimensional Materials" (J. S. Miller and A. J. Epstein Eds.) pp. 183–208. The New York Academy Sciences, New York, 1978.
12. O. Kahn, "Molecular Magnetism," VCH, New York, 1993.
13. R. Kirmse, J. Stach, W. Dietzsch, G. Steimecke, and E. Hoyer, *Inorg. Chem.* **19,** 2679 (1980).